



# Dynamic modelling of the voltage response of direct methanol fuel cells and stacks Part I: Model development and validation

A. Simoglou<sup>a</sup>, P. Argyropoulos<sup>b</sup>, E. B. Martin<sup>a</sup>, K. Scott<sup>b,\*</sup>, A. J. Morris<sup>a</sup>, W. M. Taama<sup>b</sup>

<sup>a</sup>Centre for Process Analytics and Control Technology, University of Newcastle, Merz Court, Newcastle upon Tyne, NE1 7RU, UK

<sup>b</sup>Department of Chemical and Process Engineering, University of Newcastle, Merz Court, Newcastle upon Tyne, NE1 7RU, UK

Received 6 April 2000; received in revised form 5 March 2001; accepted 17 April 2001

## Abstract

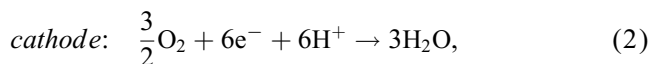
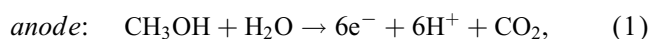
The transient response of the direct methanol fuel cell (DMFC) with liquid feed will be of particular importance in transportation applications. To achieve effective control of a commercial system it is important to develop a methodology that accurately predicts the stack voltage using a small number of sensors. An experimental study of the dynamics of the direct methanol fuel cell is described and used to develop an empirical model of the cell dynamics. Two cell systems, a small-scale single cell and a three-cell stack, form the basis of the experimental study. The cells were subjected to a range of dynamic loads and operating conditions. Empirical dynamic models were then developed, using state space canonical variates analysis, to predict the voltage response of the two systems from measurements of cell voltage and current. The models provided acceptable inferential and one-step-ahead predictions of the dynamic voltage response even though the systems never attain steady-state operation. © 2001 Elsevier Science Ltd. All rights reserved.

**Keywords:** Electrochemistry; Modelling; Dynamic simulation; Fuel cell; Voltage prediction; Transient behaviour; State space model

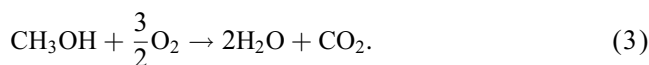
## 1. Introduction

In recent years interest in fuel cells for applications in transport and small stationary power systems, for example, has increased. This interest has primarily been as a result of the breakthrough made in polymer electrolyte membrane fuel cells (PEMFC) using hydrogen as the ‘clean’ fuel. However, the use of hydrogen raises issues concerning the safe transportation and storage of the fuel. An alternative approach is to reform/oxidise a liquid fuel to hydrogen in situ. This approach raises issues of overall system size, cost and operation. Consequently a cell that can directly oxidise a liquid fuel, e.g. methanol, methoxymethanes, formic acid, methyl formate, and ethanol is attractive. A requirement of the fuel is that, on oxidation, a clean combustion to carbon dioxide is achieved. With anticipated temperatures of operation of around 100°C, the choice with currently available electrocatalysts is limited to simple fuels such as methanol.

The direct methanol fuel cell (DMFC) based on a solid polymer electrolyte, typically operates at relatively low temperatures (< 130°C) with methanol as either vapour or liquid. The electrode reactions are



which can be combined to give the overall reaction



Research into the DMFC has generally focused on steady-state behaviour and small-scale operation with emphasis on catalyst, solid polymer electrolytes and membrane electrode assembly development (Wasmus & Kuver, 1999).

With commercialisation of DMFC technology not anticipated until around 2008, engineering aspects of the system have been largely neglected in favour of small-scale cell development. This has resulted in limited research into the dynamics of DMFC operation, in

\* Corresponding author. Tel.: 44-191-222-8771; fax: 44-191-222-5292.

E-mail address: k.scott@ncl.ac.uk (K. Scott).

particular start-up and shut-down. An investigation of the dynamics of the DMFC to assess the cell voltage response to continuously varying, or arbitrarily applied, current loads has recently been reported (Argyropoulos, Scott, & Taama, 2000a,b).

Knowledge of the dynamic behaviour of fuel cells, stacks and systems for vehicular applications is critical to their design and engineering. A number of publications have considered the dynamics of fuel cells other than the DMFC (e.g. He, 1998; Kortbeek, DeRuijter, Hagg, & Barten, 1998; Miki & Shimizu, 1998; Lee, Lalk, & Appleby, 1998; Van Bussel, Koene, & Mallant, 1998; Wohr et al., 1998; Bevers, Wohr, Yasuda, & Oguro, 1997; Amphlett, Mann, Peppley, Roberge, & Rodrigues, 1996; Hauff & Bowlin, 1995; Costamagna, Arato, Achenbach, & Reus, 1994; He, 1994a,b; Appleby, 1993). Most of these approaches were based on the deterministic modelling of experimental data and were system specific. There has been limited published data on the dynamics of the DMFC. A brief discussion of the dynamic behaviour of a small DMFC stack has been reported using current pulse operation (Valdez, Narayanan, Frank, & Chun, 1997). In a number of publications, observations on dynamics have been made, but these mainly relate to the duration of the experiments carried out on working cells (e.g. Ren, Wilson, & Gottesfeld, 1996; Hogarth & Hards, 1996; Scott, Taama, & Cruickshank, 1996; Narayanan et al., 1996a,b). The dynamics of fuel cells, in particular the DMFC, are complex and are therefore extremely challenging to model. The dynamic response of the DMFC depends on a number of factors including:

- The electrochemical response of the anode and cathode reactions.
- The charging characteristics at the interfaces between the electrode, electrolyte and solid polymer membrane.
- The mass transfer of methanol to the catalyst sites through the diffusion layer and catalyst region.
- The mass transfer of methanol through the membrane, which influences the performance of the cathode due to a mixed potential.
- The mass transfer of oxygen to the cathode.
- The production and transport of water at the cathode electrocatalyst layers.
- The production of carbon dioxide and its release from the anode catalyst layer.
- The two-phase flow of methanol solution and carbon dioxide gas through the anode diffusion layers.
- The hydrodynamics of the two-phase flow of methanol solution and carbon dioxide gas in the flow bed.
- The variation in heat release and temperature response of the cell components which affect local reaction rates, vaporisation (or condensation) of methanol (and water) between the liquid and gas phases, local humidification conditions and local operating parameters.
- The size and scale up of DMFC stacks.

The effect of many of the above factors on the dynamic response of the cell are interactive and will depend on the current load applied to the cell, the speed of load changes and the previous history of the load variations in the overall cycle imposed. The development of a deterministic model which incorporates the above factors to predict the dynamic response of the DMFC for use in cell and system control is extremely demanding. Therefore the intention of this paper is to develop an empirical dynamic model for the inference and one-step-ahead prediction of the voltage response from a limited number of sensors (voltage, current and perhaps temperature). The ultimate aim is to identify a simple and robust method for cell control. Experimental data was collected from two systems, a single small-scale DMFC and a three-cell stack (816 cm<sup>2</sup> total active area). The initial objective was to develop a model for a particular set of operating conditions for each of the two systems. The models were then validated against other data sets collected from the same system, but operated under different conditions.

The basis of the modelling work was the multivariate statistical technique of state space canonical variates analysis (CVA) (Larimore, 1983). The advantage of CVA state space modelling is that no a priori knowledge of the system parameters, dynamics, or time-delays is required. CVA was first applied to the data and pseudo-states of the system were calculated. These pseudo-states are fair approximations of the true states of the real system since they are “optimal” predictors of the future outputs. Here “optimal” implies that the prediction error is minimised. The pseudo-states were then used to develop a state space model considered as the most general representation of a linear time-invariant system. It is thus considered reasonable to use such a CVA based model to describe both the steady state and dynamic operation of the DMFC.

The overall objective of this paper is to report a CVA based model that predicts the dynamic response and that forms the basis of a control methodology for DMFC stack power trains which requires a minimal number of sensors. In the second part of the communication (Simoglou et al., 2001) the study is extended to assess the ability of the model to predict more complex scenarios, including scale-up and scale-down, where major differences in operating strategies existed. More specifically, the CVA model of the small-scale cell was used to predict the three-cell stack response and vice versa.

## 2. Experimental studies

The small-scale cell has an active cross-sectional area of 9 cm<sup>2</sup> and consists of a one membrane electrode assembly (MEA) sandwiched between two graphite blocks with flow paths cut out for methanol and oxygen/air flow. The flow bed comprises a series of 10 parallel channels, 2 mm deep × 2 mm wide every 1 mm.

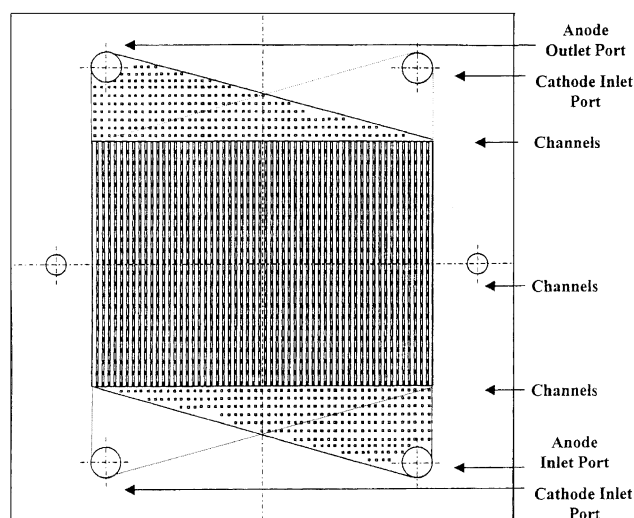


Fig. 1. Large-scale cell flow bed design.

Electrical heaters, placed behind each of the graphite blocks, heat the cell to the desired operating temperature. The graphite blocks were also provided with electrical contacts and holes to accommodate thermocouples. The fuel cell was operated in a simple flow rig which provided a temperature-controlled supply of aqueous methanol solution circulated with the aid of a peristaltic pump. Pressure regulated air was supplied from cylinders at ambient temperature. Further details of experimental equipment, MEA fabrication and operating procedures can be found in Argyropoulos, Scott, and Taama (1999).

The three-cell stack was based on a large-scale flow bed design shown in Fig. 1 (Scott, Argyropoulos, & Taama, 2000). The flow bed consists of a main flow region of 57 parallel channels and two triangular inlet/outlet sections, 40 mm long with a series of 4 mm<sup>2</sup> spots. Liquid and gas feeds and product liquid and gas mixtures are supplied/removed in an internal reverse type circular cross-section manifold. Individual cells are connected electrically in series using the graphite bipolar plates.

The fuel cell stack was operated within a flow circuit that provided a controlled rate of fuel and oxidant flow. The necessary heat load for stack start-up and for replenishing the heat losses was provided by an in-line 1.25 kW heater, controlled by an embedded thermocouple and an external PID temperature controller, that heated the methanol solution. Anode side exhaust gas and excess feed pass through a specially designed gas liquid separator. From the separator, the liquid flowed to the main reservoir where the gas was vented through a glass condenser to recover the vaporised methanol. A compressor provided the required air quantity at the desired pressure for the cathode. Two flow meters with precision valves were used to control the air supply. The cathode side exhaust gas was passed through a tank to collect the water separated from the air by a condenser on the top

of the vessel. A precision valve at the top of the condenser controlled the cathode compartment pressure. For cold start-up, the necessary heat was provided by a pair of heating plates adjacent to the two end graphite plates. Further details of experimental equipment can be found in Scott, Argyropoulos, and Taama (2000).

### 3. Direct methanol fuel cell performance and operating characteristics

In automotive applications, fuel cells can be used in hybrid configurations with, for example, batteries allowing the cells to be operated at steady state with high-power output under optimised conditions, and with the peak power demands being met by the batteries. Alternatively the fuel cells can be used as the sole power supply to minimise the vehicle's weight. The second case represents a dynamic situation in which sudden load application can be considered as the worse case scenario. Hence in the development of a model for the prediction of the voltage response, under variable load conditions, these cycles were considered as the limiting case.

A brief description of the effect of operating conditions on the voltage response of the direct methanol fuel cell (DMFC) is given in this section. At steady state, cell voltage at a fixed current density, increases with an increase in cathode air pressure and temperature of the cell and/or methanol solution. The effect of methanol concentration influences the cell voltage in several ways. First methanol concentration has a non-linear influence on anode kinetics through the complex reaction mechanism when a zero-order dependance on rate is approached at high concentrations. An increase in methanol concentration improves the mass transfer on the anode side whilst also increasing the methanol crossover to the cathode through the solid polymer electrolyte. As methanol is oxidised at the cathode side catalyst layer, a mixed potential results which reduces cell voltage. The effect of methanol solution flow rate is a complicated issue and depends on the operation of the DMFC system. In principle there are three ways of operating a DMFC cell: cold methanol solution is supplied to a continuously heated cell, preheated liquid is supplied to an unheated cell and a combination of both. Although the exact details of the processes occurring in these three cases is beyond the scope of the present text, altering the mode of operation can have a major impact on the cell voltage (Scott, Taama, Kramer, Argyropoulos, & Sundmacher, 1999). In practice however, a commercially viable DMFC would be operated with only the feed preheated (or potentially cooled) before cell entry.

In addition to the operating variables, flow bed design and its accompanying heat and gas management characteristics can cause significant variations in the cell dynamics and voltage under varying load characteristics. The

dynamic cell voltage response is significantly affected by the methanol solution flow rate, methanol concentration and cathode air pressure (Argyropoulos, Scott, & Taama, 2000a,b). Variations in voltage response are due to many phenomena, but methanol crossover from anode to cathode is a significant factor. In addition, in practical DMFC operation, the input of methanol solution at a temperature below that of the cell will cause dynamic interactions between the operating temperature of the catalyst region and methanol flow rate.

The data sets used in this study were collected under all three modes of operation listed above and over a wide range of operating conditions to examine the global nature of the model. In addition, the cells were operated over the full response region covering both the “activation” (low current) and “limiting” current regions. In this way the model developed could be applied over the whole range of the DMFC voltage response curve.

#### 4. Control requirements for solid polymer electrolyte cells

For commercialisation of the direct methanol fuel cells, it is important to develop control strategies for large multi-cell stacks installed in power automotive trains. Up to now the main application of fuel cells has been for steady-state power generation applications. “Traditional” process control techniques have been applied with relatively simple control structures. Transient operation, including start-up, shut-down and efficient transition between operating conditions, has not been a major concern compared with the optimisation of steady-state conditions. An issue that needs to be addressed is the trade-off between the complexity of control system technology and the ability to handle transient conditions. The objective is to design a control structure that keeps the measurement needs simple and leaves open the possibility of good transient control. Many of the control techniques studied are based on the installation of a large number of expensive sensors. This approach has had limited success in hydrogen-based systems. In contrast manufacturers of prototype systems now require techniques that rely on a limited number of sensors in order to reduce the system cost. In addition these sensors need to be similar, if not identical, to those currently used in modern cars. Through the identification of an acceptable control system, a balance between component performance and the initial cost of the system, which is vital for ensuring the economic viability of the new generation vehicles, might be achieved. The control architecture at both the component and system level will be model based and opens the possibility for a co-design of the cell control system and associated fault diagnosis.

Currently, for both methanol and hydrogen-based fuel cells, there is no simple, reliable and global technique

for voltage prediction. Some attempts have been made to model the system but might be described as being either system (and design) specific, or semi-empirical based on the existence of experimental data. Scott, Kraemer, and Sundmacher (1999) presented a steady-state deterministic model for the prediction of cell voltage output. This model, however, needs a large number of parameters (to be experimentally defined) and would be difficult to adopt in a simple controller unit for automotive applications. Kim, Lee, Srinivasan, and Chamberlin (1995) presented an empirical equation for voltage prediction of a hydrogen fuel cell but failed to correlate the equation constants with the system’s operating conditions. More recently this has been addressed (Scott, Kraemer, & Sundmacher, 1999) but the model still requires a significant amount of experimental effort to obtain the system parameters. Amphlett, Baumert, Mann, Peppley, and Roberge (1995) used a correlation approach based on coefficients that were dependent upon theoretical, empirical and experimental data. Such modelling approaches are not sufficiently flexible to be incorporated into programmable controllers, and are mainly system specific relying on a large number of user inputs and a large number of sensors providing on-line data.

#### 5. Canonical variate analysis-based state space modelling

Canonical variate analysis (CVA) state space modelling has previously been applied to a variety of systems. For example Peloubet, Haller, and Bolding (1990) developed a CVA state space model for the on-line adaptive model predictive control of an unstable aircraft wing flutter. Negiz, Ramanauskas, Cinar, Schlessler, and Armstrong (1998) developed statistical process monitoring tools based on a CVA state space model and applied them to a high temperature short time pasteurisation system. CVA state space modelling has also been applied to an industrial fluidised bed reactor for the prediction of the quality parameters of the system (Simoglou, Martin, & Morris, 1999). In these studies it was shown that CVA could provide a reliable representation of the underlying system.

The concept of state space modelling is based on describing a system in terms of  $k$  first-order difference equations which are combined into a first-order vector–matrix difference equation. The state space model has been widely applied in the design of control systems since the approach is multivariable and enables the inclusion of initial conditions into the analysis. A stochastic state space model, in its most general form, has been defined by Larimore (1983)

$$x_{t+1} = \mathbf{F}x_t + \mathbf{G}u_t + w_t, \quad (4)$$

$$y_t = \mathbf{H}x_t + \mathbf{A}u_t + \mathbf{B}w_t + e_t, \quad (5)$$

where  $\mathbf{x}$ ,  $\mathbf{u}$  and  $\mathbf{y}$  are the system states, inputs and outputs, respectively.  $\mathbf{F}$  ( $k \times k$ ) is the state matrix,  $\mathbf{G}$  ( $k \times nu$ ) is the input matrix,  $\mathbf{H}$  ( $ny \times k$ ) is the output matrix and  $\mathbf{A}$  ( $ny \times nu$ ) is the direct transmission matrix. The terms  $k$ ,  $nu$  and  $ny$  denote the dimension of the state, input and output spaces. The terms  $\mathbf{w}$  and  $\mathbf{e}$  denote noise processes that are assumed to be independent and identically distributed (i.i.d), with covariance matrices  $\mathbf{Q}$  and  $\mathbf{R}$  respectively. The noise  $\mathbf{B}\mathbf{w}_t + \mathbf{e}_t$  in the output Eq. (5) is correlated with the noise  $\mathbf{w}_t$  in the state Eq. (4). Larimore (1997) argued that requiring that the noise processes in Eqs. (4) and (5) to be correlated results in minimal realisation. If the state, input and output variables are known, then the state space matrices,  $\mathbf{F}$ ,  $\mathbf{G}$ ,  $\mathbf{H}$ ,  $\mathbf{A}$ ,  $\mathbf{B}$ ,  $\mathbf{Q}$  and  $\mathbf{R}$  are given by the least-squares solution, Larimore (1983).

A number of multivariate statistical algorithms have been proposed to approximate the real system states,  $\mathbf{x}$ . The most popular statistical methods for identifying state space models are partial least squares (PLS) (e.g. Simoglou, Martin, & Morris, 1999; Negiz & Cinar, 1997) and canonical variate analysis (CVA) (Larimore, 1983). The major advantage of PLS and CVA are that they define the major sources of variability in the measured variables by projecting them onto a lower dimension orthogonal subspace. This orthogonal subspace is spanned by the so-called latent variables that are linear combinations of the original process measurements. Comparing the properties of this latent space with those of the state space, the latent variables obtained from the application of PLS and CVA can be considered as a fair approximation of the states. A number of researchers have investigated and compared the application of PLS and CVA state space models (e.g. Simoglou et al., 1999; Negiz & Cinar, 1997; Juricek, Larimore, & Seborg, 1997) and have concluded that CVA outperforms PLS in terms of providing a more accurate representation of the system using fewer identified parameters. This is particularly important in real-world applications.

The approximation of the states using canonical variates analysis was proposed by Larimore (1983) based on the pioneering work of Akaike (1973). Larimore introduced the notion of the past,  $\mathbf{p}$ , and the future,  $\mathbf{f}$ , at time  $t$ :

$$\mathbf{p}(t) = [\mathbf{y}^T(t-1), \mathbf{y}^T(t-2), \dots, \mathbf{u}^T(t-1), \mathbf{u}^T(t-2), \dots]^T, \quad (6)$$

$$\mathbf{f}(t) = [\mathbf{y}^T(t), \mathbf{y}^T(t+1), \dots]^T. \quad (7)$$

The past vector,  $\mathbf{p}$ , is defined in a similar way to that of the  $\mathbf{P}$  matrix for AutoRegressive with eXogeneous (ARX) time-series variables modelling. The future vector,  $\mathbf{f}$ , includes future values of the outputs associated with time  $t$ . The problem is now one of identifying the optimal linear combinations of the past for use in “predicting” the future evolution of the process. Larimore (1983) proposed

applying canonical variates analysis between the past vector,  $\mathbf{p}$ , and the future vector,  $\mathbf{f}$ , such that the canonical variables corresponding to the vectors  $\mathbf{p}$  and  $\mathbf{f}$  are calculated so that the correlation between them is maximised. This results in good predictions of the system outputs.

In CVA two sets of parameters need to be selected, the number of past measurements required to predict the future evolution of the system and the number of CVA pseudo-states. Although the issue of model order selection has been well explored in the literature with many techniques having been proposed, in the CVA state space literature it is common practice to rely on just one criterion to select the various system orders, for example Akaike information criterion (AIC) (Akaike, 1973). In practice however, it is not advisable to rely solely on just one criterion for selecting the model. For example AIC is known to overestimate the order of an autoregressive (AR) model of finite order (Shibata, 1976). In this paper nine criteria were examined to help determine the various system orders, Akaike information criterion (AIC), final prediction error criterion (FPE), Bayesian information criterion (BIC), law of iterated logarithms criterion (LILC), normalised residuals sum of squares (NRSS), multiple correlation coefficient ( $R^2$ ), adjusted multiple correlation coefficient, ( $R_a^2$ ), Overall  $F$ -test of the loss function (OVF) and Mallow’s statistic ( $C_p$ ). A review of these model order selection criteria can be found in Haber and Unbenhauen (1990). In contrast to previous approaches to CVA state space modelling, each variable may involve a different number of past measurements to predict the response of the system (Simoglou, 1999).

## 6. Application of canonical variates analysis state space modelling to the direct methanol fuel cell

CVA state space models were developed to provide both inferential estimates (the prediction of the system output at that moment in time) and one-step-ahead predictions of the cell voltage output. The operating conditions for the experimental data sets for the two fuel cell systems are summarised in Table 1. Associated with each set of operating conditions were different loading cycles, i.e. varying patterns of applied current density, as shown in Fig. 2. Load cycles A–D relate to loadings applied to the single cell, whilst E and F were applied to the three-cell stack. Three of the load cycles (A, E and F) simulate situations that are likely to occur when driving a vehicle on a motorway, whilst load cycle B relates to the case of medium to high-power demands continuously varied with no cell relaxation (i.e. zero load). Structured loads with load pulses of various magnitudes followed by cell/stack relaxation prior to reloading were also investigated. Pulse performance as shown in Fig. 2C and D is important for many applications such as communi-

Table 1  
Operating conditions for the DMFC experiments

| Operating conditions\data set                 | Data set (A) | Data set (B) | Data set (C) | Data set (D) | Data set (E) | Data set (F) |
|---|--------------|--------------|--------------|--------------|--------------|--------------|
| Solution concentration (M)                    | 2            | 1            | 0.25         | 2            | 1            | 1            |
| Cathode pressure (bar)                        | 2            | 0.5–2        | 2            | 2            | 1.4          | 1.7          |
| Cell temperature (°C)                         | 64–71        | 79–81        | 85           | 80           | 63–71        | 43–74        |
| Methanol inlet temperature (°C)               | 80–90        | 51–54        | 50–55        | 51–57        | 66–77        | 43–76        |
| Methanol outlet temperature (°C)              | 69–79        | —            | —            | —            | 68–78        | 40–72        |
| Air inlet temperature (°C)                    | —            | —            | —            | —            | 22–23        | 21–29        |
| Air outlet temperature (°C)                   | —            | —            | —            | —            | 36–50        | 29–54        |
| Anode flow rate (cm <sup>3</sup> /min)        | 150          | 5–15         | 10           | 15           | 3500         | 5500         |
| Total active area (cm <sup>2</sup> )          | 9            | 9            | 9            | 9            | 816          | 816          |
| Number of cells                               | 1            | 1            | 1            | 1            | 3            | 3            |
| Applied current density (mA/cm <sup>2</sup> ) | 5–70         | 0–200        | 0–100        | 0–200        | 18–76        | 18–76        |
| Number of data points                         | 13912        | 9502         | 3630         | 766          | 11288        | 6908         |

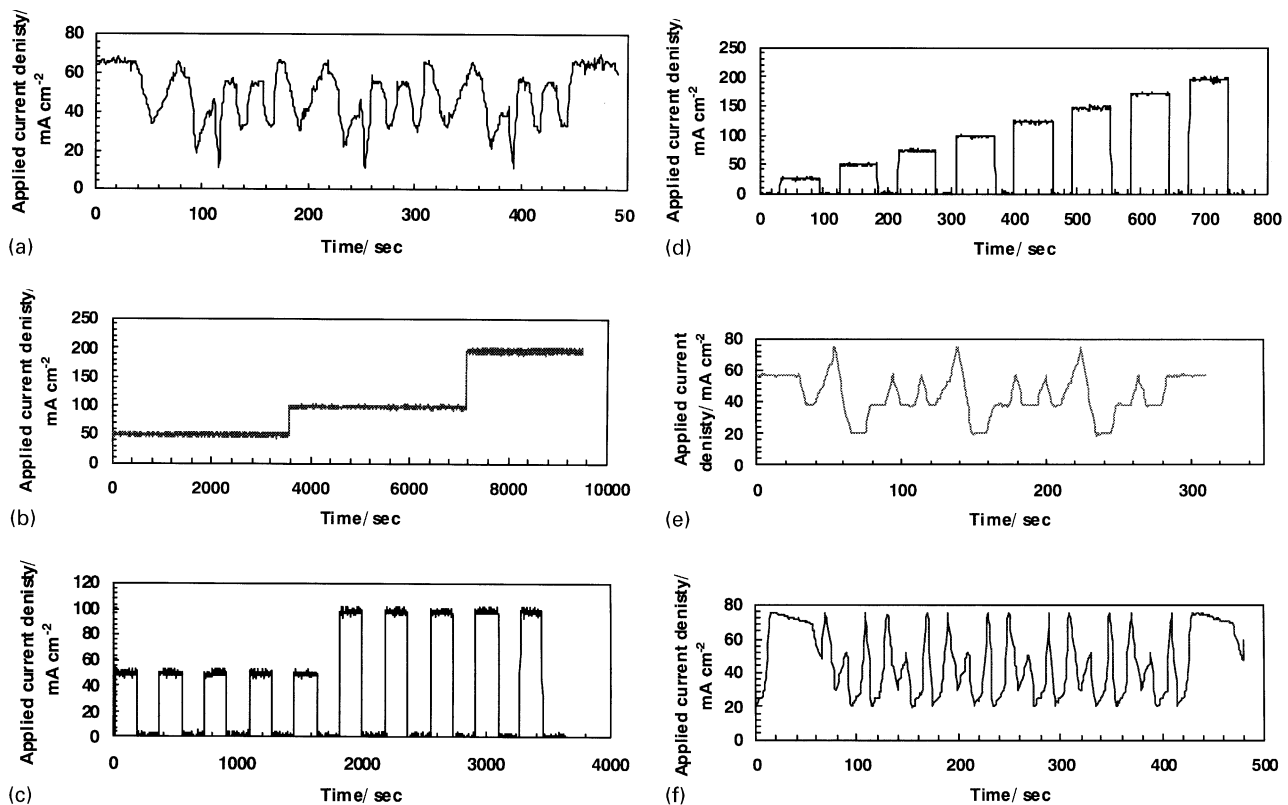


Fig. 2. Current density load cycles.

cation equipment, emergency back up power supply, and electric vehicles.

Two variables formed the basis of the dynamic empirical models. The cell/stack output voltage and the input applied load i.e. cell/stack current density. The first step in the model identification procedure was to select the number of past values required to build the CVA state space model. For the small cell, five values were required for the past values of the voltage and the current, with ten CVA pseudo-states being retained in the model. For the large-scale stack, the CVA state space model comprised

five past values of the voltage and seven past values of the current, with eleven CVA pseudo-states being retained.

The next step was to validate the assumptions associated with the output residuals,  $\mathbf{e}$ , i.e. that they are serially independent and normally distributed. Fig. 3 shows the autocorrelation function of the output residuals. From this plot, it can be concluded that the residuals were serially independent. From Fig. 4, it can be seen that the voltage prediction errors represent a zero-mean, normally distributed process thus the residuals satisfy the underlying assumptions. Based upon this assessment, it was

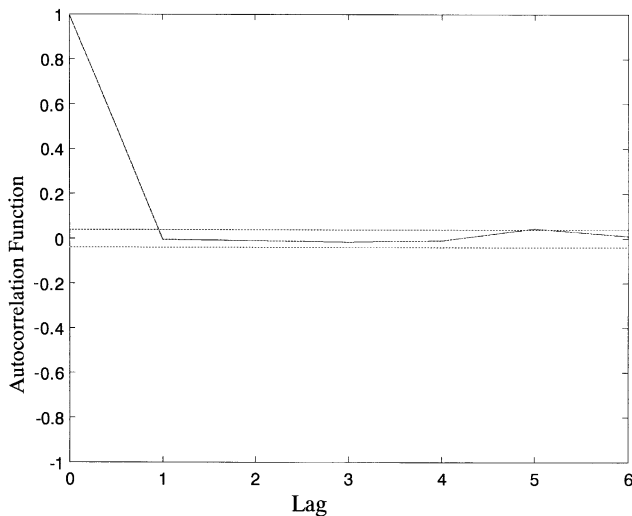


Fig. 3. Autocorrelation function of the output residuals (data set C).

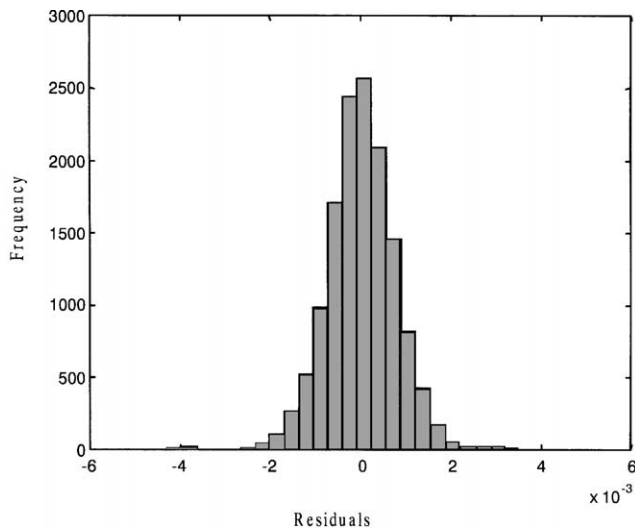


Fig. 4. Histogram of the output residuals (data set C).

concluded that the CVA state space model provided a good representation of the small DMFC. Similar results (not shown) were achieved for the three-cell large scale stack.

In model development it is important to validate the model against data sets for different operating conditions to those on which the models were built. The accuracy for the inferential estimates and one-step-ahead predictions based upon data set C are given in Table 2 for both cells. Data sets A–D relate to results for the small cell where the model was built on data set C and validated on data sets A, B and D. For the three-cell stack, the model was developed on data set F and validated on data set E. Prediction accuracy is defined as

$$\left(1 - \frac{\sum_{i=1}^n (y_i - \hat{y}_i)}{y_i}\right) \%$$

where  $y$  is the actual measured value,  $\hat{y}$  is the estimated value and  $n$  is the number of data points. The model accuracy for the inferential estimates is high with values being in excess of 96% for all data sets. Compared to the inferential estimates, the prediction accuracy for the one-step ahead predictions were poorer by between 0.23% and 1.77%. In general the differences in all the results can be attributed to the differences in the experimental conditions.

Initially the study focussed on data-set (A), generated from the small-scale DMFC cell. Previous studies on this cell (Argyropoulos, Scolt, & Taama, 1999) have identified relatively poor heat transfer characteristics and significant gas management problems. The cell was operated with preheated feed only. The elevated cathode pressure coupled with the 2.0 M aqueous methanol solution used enhanced the response of the cell to variations in the applied load. Fig. 5 is a plot of the inferential estimates versus the actual values for data set (A) with Fig. 6 providing the resulting time-series plot for data set (A) based on the model developed from data set (C). Figs. 7 and 8 show scatter plots of the one-step-ahead predictions and the actual values and the time-series plot of the one-step-ahead predictions, respectively. The results demonstrate that the model gives acceptable predictions even though the cell was not operated under steady state conditions, i.e. it had not reached steady state thermal conditions. This is in contrast to the constant cell temperature in the case of reference data set (C). The more concentrated methanol solution, 2.0 M (as opposed to 0.25 M for data set (C)) was expected to enhance the methanol crossover through the polymer electrolyte membrane rate leading to greater cathode side polarisation and thus reducing the cell voltage and slowing the dynamic response, whilst improving anode side mass transfer. The relative balance between these two mechanisms was found to dictate cell response time (Argyropoulos et al., 2000a). Increasing the liquid phase flow rate by an order of magnitude in data set (A), was expected to have less of an impact on dynamic response since it enhanced gas removal compared to that with the lower flow rate used for data set (C). At the same time lowering the reactants supply rate increases the cell response time (a gas blanket can form on the surface of the MEA which can lower the reactants penetration rate).

The second data set, (B), relates to the small-scale cell heated to 80°C with a 1.0 M methanol solution at 51–54°C (the feed was not preheated). Initially the cell was operated with low air flow rate and pressure resulting in cathode flooding which causes the performance of the cell to deteriorate rapidly (Valdez, Narayanan, Frank, & Chun, 1997). In practice every time a water droplet was flushed from the cell, a large fall in cell voltage was recorded. This behaviour is observed in Fig. 9. These points are those that lie away from the 45° diagonal. Fig. 10 illustrates the resulting inferential estimates for data set (B) for the case where the results were developed from the

Table 2  
Accuracy of inferential estimates and one-step-ahead predictions of the six data sets

|                                | Data set (A) | Data set (B) | Data set (C) | Data set (D) | Data set (E) | Data set (F) |
|--------------------------------|--------------|--------------|--------------|--------------|--------------|--------------|
| Inferential estimates (%)      | 96.60        | 97.53        | 98.25        | 96.53        | 99.39        | 99.15        |
| One-step-ahead predictions (%) | 95.41        | 96.65        | 98.02        | 94.76        | 98.99        | 98.64        |

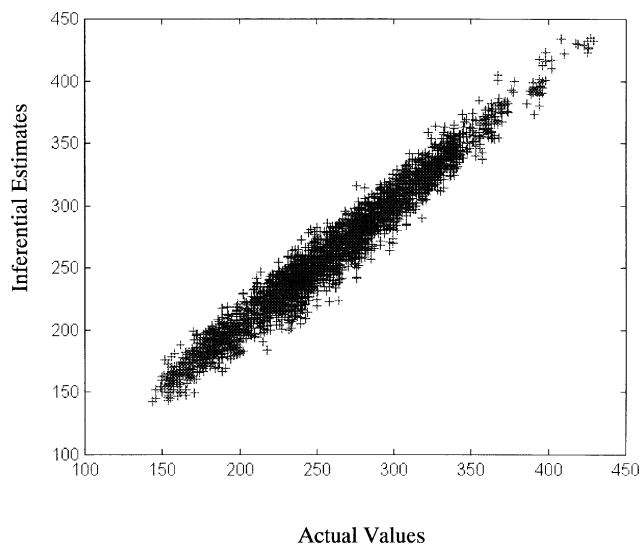


Fig. 5. Actual values versus inferential estimates for data set (A).

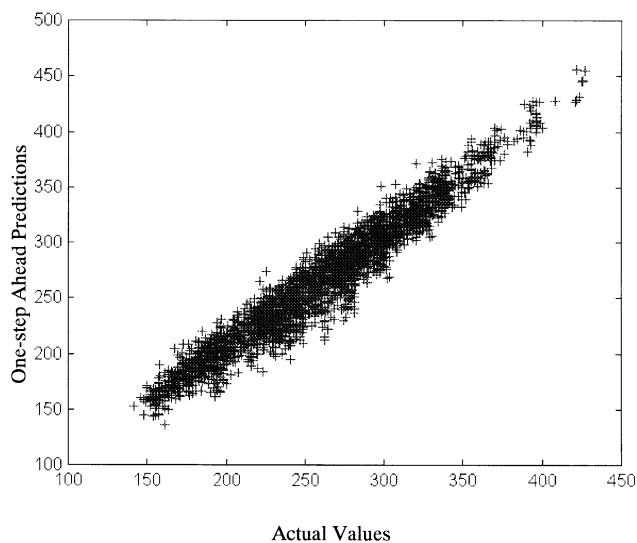


Fig. 7. Actual values versus one-step-ahead predictions for data set (A).

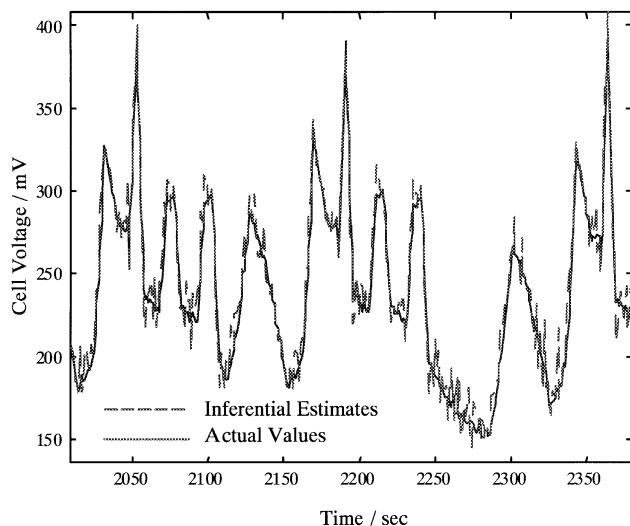


Fig. 6. Inferential estimates of data set (A).

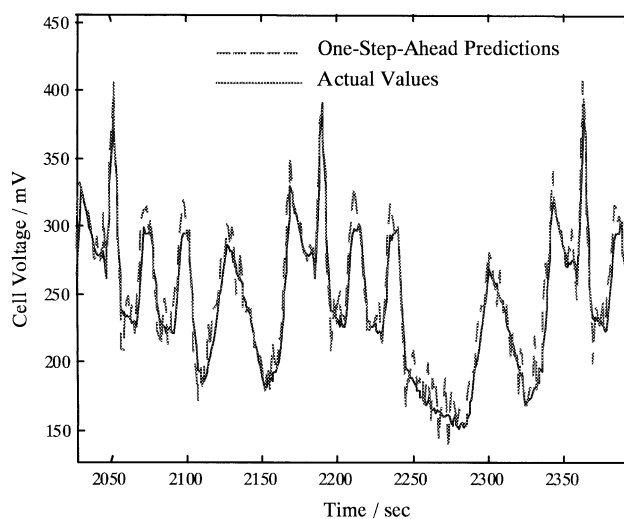


Fig. 8. One-step-ahead predictions of data set (A).

model built using data set (C). The results are acceptable even though clear differences exist between the two sets of operating conditions. During the experiment, the anode side flow rate and the applied load were changed three times and the cathode pressure was changed four times. The cell was operating in an unstable mode, with significant voltage variations and step changes in operating conditions; cathode side pressure was varied from

the initial value of 0.5 bar to the final value of 2.0 bar and the anode side inlet flow rate was varied over a range of 5 to 15 cm<sup>3</sup> min<sup>-1</sup>. A 1.0 M methanol concentration was found to optimise the specific cell dynamic response (Argyropoulos, Scott, & Taama, 2000a) and gives a significantly shorter response time compared with the dilute 0.25 M solution used for data set (C). Finally the applied



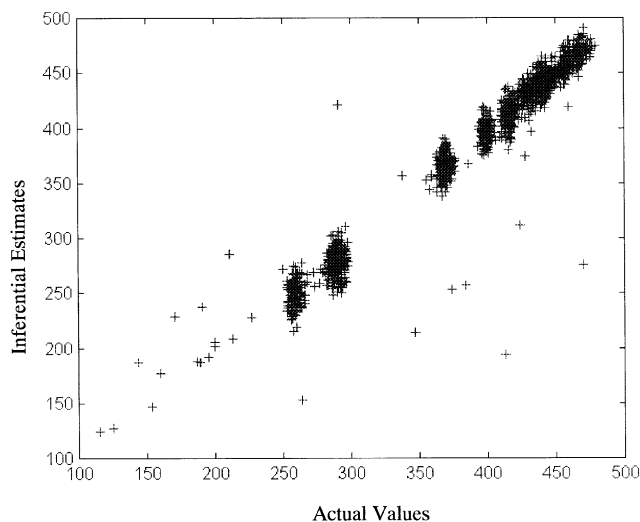


Fig. 9. Actual values versus inferential estimates for data set (B).

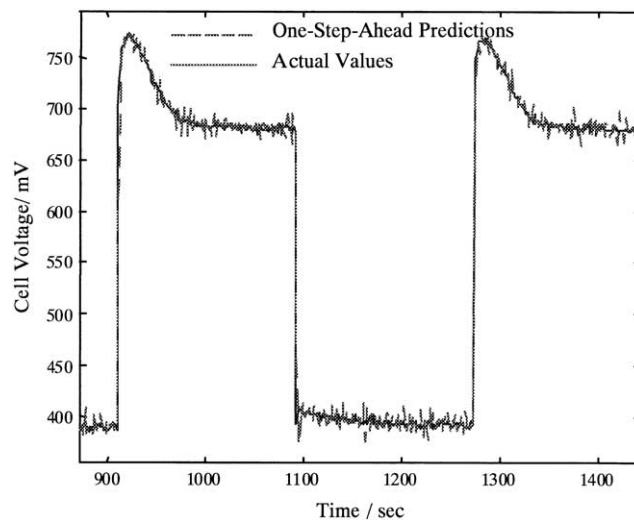


Fig. 11. One-step-ahead predictions of data set (C).

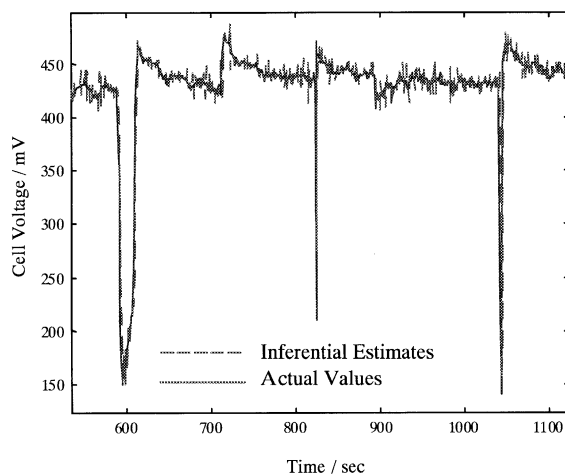


Fig. 10. Inferential estimates of data set (B).

current density range increased from 0 to  $100 \text{ mA cm}^{-2}$ , for data set (C), to 0 to  $200 \text{ mA cm}^{-2}$ , for data set (B). The one-step-ahead predictions generated for data set B, using the model built on data set (C), exhibited very similar behaviour to that shown in Fig. 10.

The third data set, (C), is particularly challenging from two aspects: (i) the methanol solution used is dilute (0.25 M) which leads to a relatively slow voltage response especially at higher current densities where the cell suffers from mass transfer limitations, and (ii) it had been found from previous studies (Argyropoulos et al., 2000a,b) that cell relaxation (i.e. cell unloading between two successive load applications) significantly affects the cell response, i.e. the cell voltage rises to levels greater than the initial (or steady state) open-circuit voltage. The third and the fourth data sets (C and D) are worst case scenarios as they represent sudden applications of various power demands. In general such variations in

load, i.e. current density, would not be imposed on a cell or stack used for automotive applications. In driving cycles currently used for car certification world wide, the demands on an automotive power source are more relaxed. It is not a prerequisite of the power source to respond to pulses from zero-load to, 50–75%, of the maximum power output. On the other hand such cases provide a challenging way to test the system. The model predictions for data set (C), Table 2, for the inferred predictions (98.25%) and the one-step-ahead predictions (98.02%) are, as expected, adequate since this data set was used to build the model. The agreement between model one-step-ahead predictions and experimental data is shown in Fig. 11. This behaviour is also reflected in the scatter plot of the actual values versus the inferential predictions and the one-step-ahead results (not shown).

Consider now the predictions for data set D from the model built from data set (C). The difference between data sets (C) and (D) lies in the cell relaxation time, i.e. the time interval without load between two successive loading periods. In data set (D), the time interval was reduced from 180 to 30 s. The implication of this is that, in the case of data set (D), the physical processes of mass and heat transfer, and gas removal may not have reached a steady state before the next pulse is applied. In addition data set (D) includes a large number of system excitations over a wider range of current densities (0– $200 \text{ mA cm}^{-2}$ ) compared with the two different excitations at 50 and  $100 \text{ mA cm}^{-2}$  used for data set (C). It has previously been shown that the cell response pattern is significantly affected by the magnitude of the applied current density (Argyropoulos et al., 2000b). Overall, considering that the solution concentration is higher compared to the reference data set (2.0 M versus 0.25 M), the flow rate is higher and the cell temperature is lower,

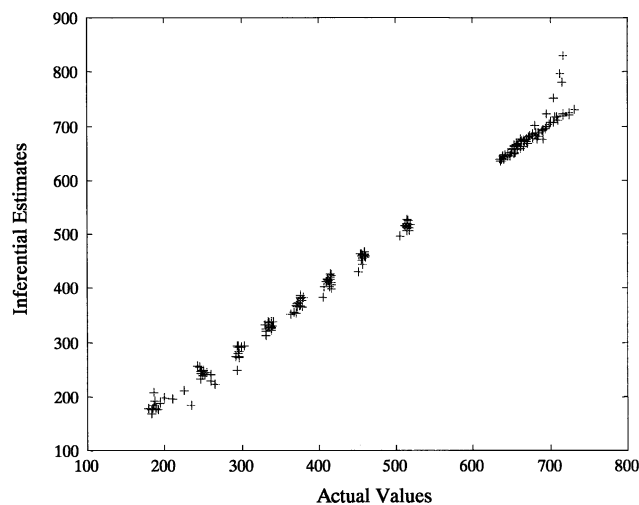


Fig. 12. Actual values versus inferential estimates for data set (D).

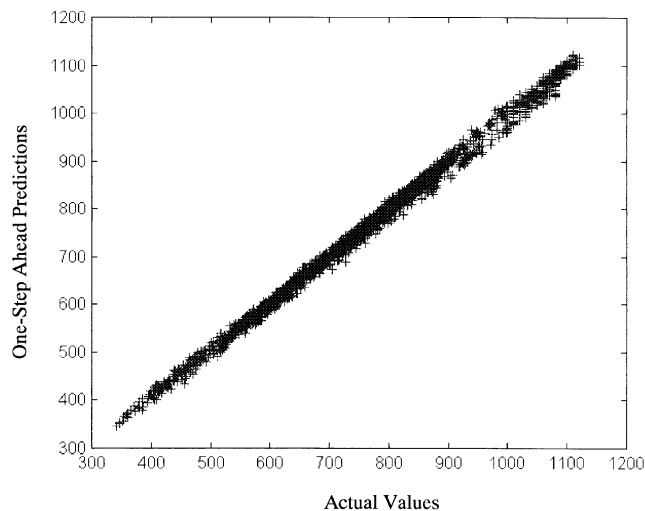


Fig. 14. Actual values versus one-step-ahead predictions for data set (E).

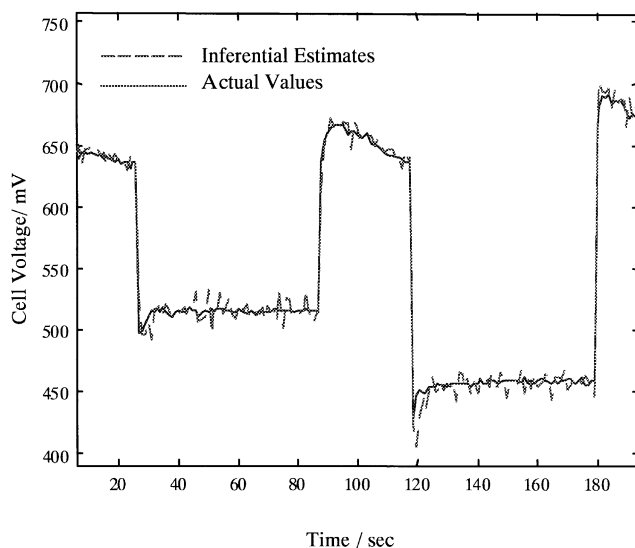


Fig. 13. Inferential estimates of data set (D).

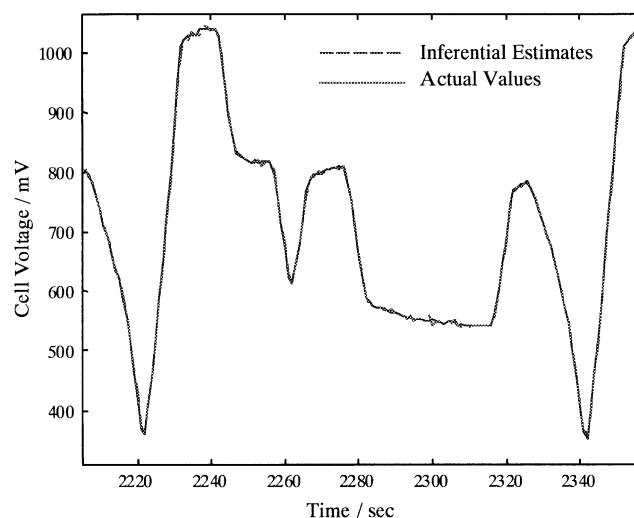


Fig. 15. Inferential estimates of data set (E).

the resulting model predictions are more than satisfactory. This is illustrated in Figs. 12 and 13 for the inferential estimates. Similar behaviour was observed for the one-step-ahead predictions (not shown).

Two data sets (E and F) were collected from the three-cell stack. Due to the differences in cell design, a separate CVA model was generated from data set (F) and was validated against data set (E). The feed was a 1.0 M aqueous methanol solution for both experiments. Flow, current and pressure distribution, gas and thermal management, are problems that are less significant with the small cell than the cell stack. Stack dynamics, especially heat and mass transfer processes, are also at least an order of magnitude slower than the fast electrochemical processes taking place inside the membrane electrode assembly (MEA). It should be noted that the DMFC

typically operates between 70 and 100°C and rarely is operational at temperatures less than 60°C. Nevertheless, for automotive applications, a model for voltage prediction should be able to predict voltages during cold start-ups. The results plotted for data sets E and F (Figs. 14–16) demonstrate the ability of the model to track changes between operating and loading conditions. Another interesting feature is that the cell is continuously loaded for prolonged time intervals and in general the system is operated under unfavourable conditions. This is exemplified by the ambient temperature being quite low (5°C) and the stack being loaded without allowing the membrane electrode assembly to reach a temperature that will enhance the reaction kinetics.

From Table 2, the model predictions for data sets (E) and (F) have accuracies in excess of 98% for both the inferential and one-step-ahead predictions. The scatter plot

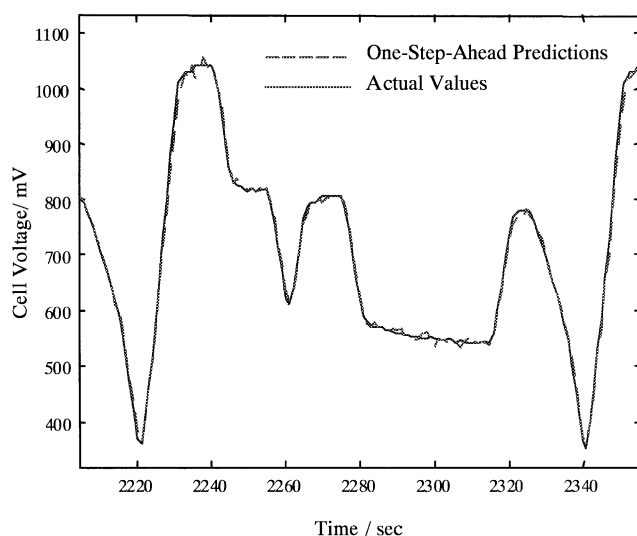


Fig. 16. One-step-ahead predictions of data set (E).

for data set (E) in Fig. 14 for the one-step-ahead predictions confirms these good predictions as does the corresponding plot for the inferential estimates (not shown). Typical time-series plots are given in Fig. 15 for the inferential estimates and Fig. 16 for the one-step-ahead predictions for data set (E). Similar conclusions to those for the response of the small cell can be drawn concerning the ability of the three cell stack model to give good quality predictions irrespective of the large changes in system operating conditions.

## 7. Conclusions

Overall this feasibility study has highlighted the potential of state space CVA dynamic modelling for fuel cell voltage predictions. This investigation has revealed the flexibility of the methodology for predicting, with good accuracy, the voltage response of DMFC's systems under both steady state and dynamic conditions and with changes in conditions during operation. One key issue is that of obtaining the data set on which the model is to be built. In the present study the data sets were generated from experiments conducted as a general investigation into the dynamic response of DMFC and hence these experiments were not specifically designed for model building. It is conjectured that the accuracy of the models would be significantly increased if data from specially designed experiments had been used as the reference data set.

It is generally accepted that the voltage response of a fuel cell strongly depends on the applied current density and to a lesser extent on variations in cell operating conditions. Nevertheless, as fuel cell technology moves towards large-scale systems and to wide variations in terms

of operating conditions, these characteristics need to be incorporated within the CVA model structure to improve accuracy. Two possible solutions are (i) to build a model for a specific system from a large data set and achieve relatively high accuracy predictions but with minimal sensor requirements, and (ii) to increase model accuracy by using more sensor information which implies penalties in terms of increased cell instrumentation. An important issue in state space CVA model development is the prediction accuracy when CVA models developed from different systems are used to predict the voltage output of scaled-up or scaled-down systems and multi-cell stacks. This issue is addressed in the second part of this communication (Simoglou et al., 2001).

## Acknowledgements

The authors would like to acknowledge the following for support of this research: the EPSRC Innovative Manufacturing Initiative Award, SCIENTIA (GR/L28029) for supporting Dr. A. Simoglou; the European Commission for a TMR Marie Curie B20 research-training grant to Dr. P. Argyropoulos; the EPSRC for support of Dr. W. M. Taama; and Johnson Matthey Technology Centre for the supply of developmental catalyst under their catalyst loan scheme.

## References

- Akaike, H. (1973). Information theory and an extension of the maximum likelihood principles. *Proceedings of the second international symposium on information Theory*, Budapest.
- Amphlett, J. C., Baumert, R. M., Mann, R. F., Peppley, B. A., & Roberge, P. R. (1995). Performance modelling of the Ballard Mark IV solid polymer electrolyte fuel cell. *Journal of the Electrochemical Society*, 142(1), 1–8, 9–15.
- Amphlett, J. C., Mann, R. F., Peppley, B. A., Roberge, P. R., & Rodrigues, A. (1996). A model predicting transient responses of proton exchange membrane fuel cells. *Journal of Power Sources*, 61, 183–188.
- Appleby, A. J. (1993). Characteristics of fuel cells systems. In: L. J. M. Blomen, M. N. Mugerwa (Ed.), *Fuel cell systems* (pp. 157–173). New York: Plenum Press.
- Argyropoulos, P., Scott, K., & Taama, W. M. (2000a). The effect of operating conditions on the dynamic response of the direct methanol fuel cell. *Electrochimica Acta*, 45, 1983.
- Argyropoulos, P., Scott, K., & Taama, W. M. (2000b). Dynamic response of the direct methanol fuel cell under variable load conditions. *Journal of Power Sources*, 87, 153.
- Argyropoulos, P., Scott, K., & Taama, W. M. (1999). Gas evolution and power performance in direct methanol fuel cells. *Journal of Applied Electrochemistry*, 29, 661–669.
- Bevers, D., Wöhr, M., Yasuda, Y., & Oguro, K. (1997). Simulation of a polymer electrolyte fuel cell electrode. *Journal of Applied Electrochemistry*, 27, 1254–1264.
- Costamagna, P., Arato, E., Achenbach, E., & Reus, U. (1994). Fluid dynamic study of fuel cell devices: Simulation and experimental validation. *Journal of Power Sources*, 52, 243–249.

- Haber, R., & Unbenhauen, H. (1990). Structure identification of non-linear dynamic systems—A survey on input–output approaches. *Automatica*, 26(4), 651–677.
- Hauff, S., & Bowlin, K. (1995). Thermal relaxation during dynamic fuel cell operation. *Journal of Power Sources*, 55(2), 167–176.
- He, W. (1994a). A simulation model for integrated fuel cell systems. *Journal of Power Sources*, 49(1–3), 283–290.
- He, W. (1994b). The dynamic performance of a molten-carbonate fuel cell in power generation systems. *Journal of Power Sources*, 52(2), 179–184.
- He, W. (1998). An investigation on the dynamic performance of molten carbonate fuel-cell power-generation systems. *International Journal of Energy Research*, 22(4), 355–362.
- Hogarth, M. P., & Hards, G. A. (1996). Direct methanol fuel cells. Technological advances and further requirements. *Platinum Metals Review*, 40(4), 150–159.
- Juricek, B. E., Larimore, W. E., & Seborg, D. E. (1997). Reduced-Rank ARX and subspace system identification for process control. *DYCOPS-5, Proceedings of the fifth IFAC symposium on dynamics and control of process systems* (pp. 245–250).
- Kim, J., Lee, S., Srinivasan, S., & Chamberlin, C. E. (1995). Modeling of proton exchange membrane fuel cell performance with an empirical equation. *Journal of Electrochemical Society*, 142(8), 2670–2674.
- Kortbeek, P. J., DeRuijter, J. A. F., Hagg, V. P. C. F., & Barten, H. (1998). A dynamic simulator for a 250 kW class ER-MCFC system. *Journal of Power Sources*, 71(1,2), 278–280.
- Larimore, W. E. (1983). System identification, reduced order filtering and modeling via canonical correlation analysis. *Proceedings of the American Control Conference* (pp. 445–451).
- Larimore, W. E. (1997). Canonical variate analysis in control and signal processing. In K. Katayama & S. Sugimoto (Eds.), *Statistical methods in control and signal processing*. (pp. 83–120). New York: Marcel Dekker.
- Lee, J. H., Lalk, T. R., & Appleby, A. J. (1998). Modelling electrochemical performance in large scale proton exchange membrane fuel cell stacks. *Journal of Power Sources*, 70, 258–268.
- Miki, H., & Shimizu, A. (1998). Dynamic characteristics of a phosphoric acid fuel cell. *Applied Energy*, 61(1), 41–56.
- Narayanan, S. R., Halpert, G., Chun, W., Jeffries-Nakamura, B., Valdez, T. I., Frank, H., & Surampudi, S. (1996a). The status of direct methanol fuel cell technology at JPL. *Proceedings of the 37th power sources conference*, Cherry Hill, NJ, USA.
- Narayanan, S. R., Halpert, G., Chun, W., Jeffries-Nakamura, B. T. I., Valdez, H., Frank, H., & Surampudi, S. (1996b). Recent advances in the performance of direct methanol fuel cells. *Electrochemical society annual meeting*, Los Angeles, CA, USA.
- Negiz, A., & Cinar, A. (1997). PLS, balanced and canonical variate realisation techniques for identifying VARMA models in state space. *Chemometrics and Intelligent Laboratory Systems*, 38, 209–221.
- Negiz, A., Ramanauskas, P., Cinar, A., Schlessler, J. E., & Armstrong, D. J. (1998). Modeling, monitoring and control strategies for high temperature short time pasteurization systems. Statistical monitoring of product lethality and process sensor reliability. *Food Control*, 9(1), 29–47.
- Peloubet, R. P., Haller, R. L., & Bolding, R. M. (1990). On-line adaptive control of unstable aircraft wing flutter. *Proceedings of the 29th conference on decision and control*, Hawaii, Vol. 1 (pp. 643–651).
- Ren, X., Wilson, M. S., & Gottesfeld, S. (1996). High performance direct methanol polymer electrolyte fuel cells. *Journal of the Electrochemical Society*, 143(1), L12–L15.
- Scott, K., Argyropoulos, P., & Taama, W. M. (2000). Modelling transport phenomena and performance of direct methanol fuel cell stacks. *ICHEME Transactions*, 78, 881.
- Scott, K., Kraemer, S., & Sundmacher, K. (1999). Gas and liquid mass transport in solid polymer electrolyte fuel cells. *Proceedings of the fifth European symposium on electrochemical engineering*, Exeter. UK: IChemE.
- Scott, K., Taama, W. M., & Cruickshank, J. (1996). Performance and modelling of a direct methanol solid polymer electrolyte fuel cell. *Proceedings of the Fourth European symposium on electrochemical engineering: Contemporary trends in electrochemical engineering*, Prague (pp. 28–30). August 1996.
- Shibata, R. (1976). Selection of the order of an autoregressive model by Akaike's information criterion. *Biometrika*, 63, 117–126.
- Simoglou, A. (1999). *Chemical & process engineering*. Ph.D. thesis. University of Newcastle, Newcastle upon Tyne.
- Simoglou, A., Argyropoulos, P., Martin, E. B., Scott, K., Morris, A. J., & Taama, W. M. (2001). Dynamic modelling of the voltage response of direct methanol fuel cells and stacks. Part II. Feasibility study of model-based scale-up and scale-down. *Chemical Engineering Science*, 56, 6773–6779.
- Simoglou, A., Martin, E. B., & Morris, A. J. (1999). A comparison of canonical variate analysis and partial least squares for identifying dynamic processes. *Proceedings of the American control conference*. San Diego.
- Wasmus, S., & Kuver, A. (1999). Methanol oxidation and direct methanol fuel cells: A selective review. *Journal of Electroanalytical Chemistry*, 461, 4–31.
- Wohr, M., Bolwin, K., Schnurnberger, K., Fischer, M., Neubrand, W., & Eigenberger, G. N. (1998). Dynamic modelling and simulation of a polymer membrane fuel cell including mass transport limitation. *International Journal of Hydrogen Energy*, 23(3), 213–218.
- Valdez, T. I., Narayanan, S. R., Frank, H., & Chun, W. (1997). Direct methanol fuel cell for portable applications. Annual battery conference on applications and advances. Long Beach, USA.
- Van Bussel, H. P. L. H., Koene, G. H., & Mallant, R. K. A. M. (1998). Dynamic model for solid polymer fuel cell water management. *Journal of Power Sources*, 71, 218–222.